sustainability

MDPI

Article

Investigation of Dynamic Characteristics of Liquid Nitrogen Droplet Impact on Solid Surface

Ke Zhao [1] and Yang Ding [2,*]

[1] School of Biology and Food Engineering, Chuzhou University, Chuzhou 239000, China; spzk@chzu.edn.cn
[2] School of Mathematics and Finance, Chuzhou University, Chuzhou 239000, China
* Correspondence: sxdy@chzu.edu.cn; Tel.: +86-178-5500-0234

Abstract: Liquid nitrogen spray cooling technology exhibits excellent heat transfer efficiency and environmental protection performance. The promotion of this technology plays an important role in improving the sustainable development of the refrigeration industry. In order to clarify its complex microscale behavior, the coupled Level Set-VOF method was adopted to study the dynamic characteristics of liquid nitrogen droplet impact on solid surface in this paper. The spreading behaviors under various factors (initial velocity, initial diameter, wall temperature, and *We* number) were systematically analyzed. The results show that the spreading behaviors of liquid nitrogen droplet share the same process with the normal medium, which are rebound, retraction, and splashing. For the droplet with smaller velocity and diameter, Rebound is the common phenomenon due to the smaller kinetic energy. With the increase of droplet diameter (0.2 mm to 0.5 mm) and velocity (0.1 m/s to 5 m/s), the spreading factor increases rapidly and the spreading behaviors evolve into retraction and splashing. The increase of wall temperature accelerates the droplets spreading, and the spreading factor increases accordingly. For the liquid nitrogen droplets hit the wall, the dynamic behaviors of rebound ($We < 0.2$), retraction ($0.2 < We < 4.9$), and splashing ($We > 4.9$) will occur with the droplet weber number increased, which are consistent with the common medium. However, due to liquid nitrogen having lower viscosity and surface tension, the conditions of morphological transformations are different from the common media. The maximum spreading diameter has a power correlation with *We*, the power index of *We* is 0.306 for liquid nitrogen, lager than common medium (0.25). The reasons are: (1) the better wettability of liquid nitrogen, and (2) the vapor generated by the violent phase change ejects along the axial direction. The article will provide a certain theoretical basis for liquid nitrogen spray cooling technology, and can also enrich the flow dynamics of cryogenic fluids.

Keywords: droplet impingement; liquid nitrogen; Level Set-VOF simulation

check for updates

Citation: Zhao, K.; Ding, Y. Investigation of Dynamic Characteristics of Liquid Nitrogen Droplet Impact on Solid Surface. *Sustainability* **2022**, *14*, 710. https://doi.org/10.3390/su14020710

Academic Editors: Yuehong Lu, Changlong Wang and Zafar Ali Khan

Received: 19 November 2021
Accepted: 21 December 2021
Published: 9 January 2022

Publisher's Note: MDPI stays neutral with regard to jurisdictional claims in published maps and institutional affiliations.

Copyright: © 2022 by the authors. Licensee MDPI, Basel, Switzerland. This article is an open access article distributed under the terms and conditions of the Creative Commons Attribution (CC BY) license (https://creativecommons.org/licenses/by/4.0/).

1. Introduction

The main reasons that traditional refrigerants cause global warming are the emissions of CO_2 and fluorocarbons [1,2]. Liquid nitrogen, as a cooling medium with low boiling point, large latent heat, high cooling rate, and high development value, is widely used in low-temperature environment simulations such as biomedicine, food freezing, and low-temperature wind tunnels by the method of spray cooling. Importantly, compared with traditional refrigerants, its non-polluting characteristics cause the liquid nitrogen spray cooling technology to show an obvious advantage in terms of sustainable development.

Spray cooling involves the impact of droplets on the wall, the interaction between the droplets, and the droplets hitting the liquid film, which is a complex multiphase flow problem [3]. When the temperature of the wall is higher than the droplet fluid Leidenfrost temperature point (T_{DL}), the droplet instantly evaporates after contacting the wall surface and generates a stable vapor film between the bottom of the droplet and the wall surface [4]. The Leidenfrost effect severely impairs the performance of spray cooling,

which is particularly significant for spray cooling with liquid with low boiling point, such as liquid nitrogen.

In fact, studying the spreading dynamics and evaporation heat transfer process of the single droplet impinging on the wall is the basis of the investigation of the two-phase heat transfer mechanism in spray cooling technology. The single droplet impacting wall surface has been widely used for prediction of spray impingement. Many scholars have carried out numerous studies on the thermodynamic characteristics of liquid droplets hitting walls by the methods of theoretical analysis [5], experimental research [6–10], and numerical simulation [11]. The droplet impinging on wall surface is a multi-scale and strong transient process. The surface temperature directly affects the characteristic size and splash threshold of the secondary droplets [12]. Wachters [6] studied the process of water droplets impacting high-temperature polished metal surfaces, and believed that the Leidenfrost effect would occur only when the wall temperature was higher than 443 K; however, Baumeister and Simon [7] found that the Leidenfrost phenomenon occurs only when the wall temperature was higher than 543 K for the water droplets. In addition, droplet properties (cryogens, hydrocarbons, and water), diameter, and velocity also have important effects. Scheller and Bousfield [8] used the liquid of glycerin-water mixtures to study the influencing factors such as initial diameter, initial velocity, and wall type, and obtained the empirical formula of the maximum dimensionless wetting length when the droplet does not retract. Liu et al. [9] used carbon nanotubes, graphene, and nano-graphite powder to prepare three kinds of stable nanofluids, and captured the dynamic process of the three nanofluids impacting the solid wall by micro high-speed digital camera technology. The results showed that all three kinds of nanoparticles could promote the liquid to show significant shear thinning characteristics, and the shear viscosity of the fluid played an important role in the expansion process of the droplets hitting the wall surface; the dimensionless height and spreading factor of droplets were negatively correlated with the shear viscosity of nanofluids. Tuan et al. [10] used a high-speed camera to photograph the process of water drop ($0.5 \leq We \leq 500$) impacting a high-temperature smooth wall ($523\ \mathrm{K} \leq T \leq 833\ \mathrm{K}$), showing three different mechanisms: contact boiling, mild film boiling, and atomized film boiling; the dimensionless maximum spreading factor of droplets under the mild film boiling and atomizing film boiling regions were directly proportional to $We^{2/5}$, and T_{DL} increased as *We* increased; the transition temperature from mild film boiling to atomized film boiling was related to the bubble in the liquid film, and the transition temperature decreased as *We* increased.

In current studies on the dynamic characteristics of droplets impacting the wall, the influence of droplet initial diameter, initial velocity [8], wall temperature [10], contact time, and wall micro-morphology [6] on the dynamic characteristics are studied based on dimensionless diameter, dimensionless time [13], dynamic Leidenfrost temperature [14], characteristic number *Re*, and *We* [15]. The droplet medium is mainly focused on water, ethanol solution, diesel, butane, and FC-72. Conversely, there are few reports about the impact of low-temperature fluid droplets on the wall surface [16,17]. Studying the process of liquid nitrogen droplets impinging on the wall surface not only enriches the gas-liquid heat transfer theory, but also has a positive significance for guiding the practical research of liquid nitrogen spray cooling.

In this paper, a coupled Level Set-VOF(CLSVOF) phase interface tracking method was used to establish a calculation model of single liquid nitrogen droplet hitting a horizontal wall surface. The spreading characteristics of liquid nitrogen droplets are investigated with different initial diameters and initial velocities. The spreading state of droplets under the multiple factors are analyzed and compared with the ordinary fluids. This article explores the impact dynamics characteristics of liquid nitrogen droplets under various working conditions from a microscopic point of view, which has a certain reference value for deepening the understanding of the liquid nitrogen spray cooling process. It is beneficial to enhance the working fluid utilization rate and increase the heat exchange performance of the liquid nitrogen spray cooling.

2. Numerical Method and Model Validation

2.1. Numerical Method

The methods of VOF and Level Set have disadvantages such as low computational convergence, stability, and accuracy [17,18]. The tracking accuracy of the phase interface can be improved by using the CLSVOF method [19]. The calculation process of CLSVOF method includes the following steps: initialization of phase function, solution of flow control equation, solution of convection transport equation of phase function, reconstruction of phase interface, and re-initialization of phase function. The CLSVOF method constructs the phase interface through the functions of ϕ and F together (the F function represents the volume fraction of the liquid occupying the space in the calculation cell. The algebraic value of ϕ to distinguish the phases in the calculation area), adopts the piecewise linear interface reconstruction idea, and moves the interface in the normal direction so that the area ratio of the liquid region of the element matches the F function value, the vertical distance from the element center to the phase interface is obtained by iteratively solving the secant method. The calculation method of interface normal vector $\boldsymbol{n}$ is as follows:

$$\boldsymbol{n} = \frac{\nabla \phi}{|\nabla \phi|}, \tag{1}$$

The interface curvature $\kappa(\phi)$ is given by:

$$\kappa(\phi) = \nabla \bullet \frac{\nabla \phi}{|\nabla \phi|}, \tag{2}$$

Convection transport equation:

$$\frac{\mathrm{D}F}{\mathrm{D}t} = \frac{\partial F}{\partial t} + (\boldsymbol{u} \bullet \nabla) F = 0, \tag{3}$$

$$\frac{\mathrm{D}\phi}{\mathrm{D}t} = \frac{\partial \phi}{\partial t} + (\boldsymbol{u} \bullet \nabla) \phi = 0, \tag{4}$$

where $\boldsymbol{u}$—is the velocity of fluid (m/s).

After solving the convection transport equation, the ϕ function will no longer maintain the figure of the distance function. Therefore the ϕ function must be re-initialized. Re-initialization mainly includes the determination of ϕ function symbols and ϕ function values. The ϕ function value is the minimum distance from the center of the element to the phase interface, and the symbol of the ϕ function is determined by the value of the F function:

$$S^{\phi} = \mathrm{sign}(0.5 - F), \tag{5}$$

If $F < 0.5$, the unit center is in the gaseous region, and the ϕ function is positive. If $F > 0.5$, the unit center is in the liquid region, and the ϕ function is negative. If $F = 0.5$, $\phi = 0$, it indicates the phase interface, sign() is a symbolic function.

2.2. Governing Equation

2.2.1. Continuity Equation and Momentum Equation

This involves solving the governing equations to obtain a discrete quantitative description of the flow field. The governing equations of two phase (gas-liquid) flow mainly include continuity equation and momentum equation:

$$\nabla \bullet \boldsymbol{u} = 0, \tag{6}$$

$$\begin{aligned} \rho(\phi)(\partial \boldsymbol{u}/\partial t + \boldsymbol{u} \bullet \nabla \boldsymbol{u}) = \\ -\nabla p - \boldsymbol{F_s} + \nabla \bullet \boldsymbol{\tau} + \rho(\phi) \boldsymbol{g} \end{aligned}, \tag{7}$$

ρ—density (kg/m^3),
p—pressure (Pa),

$\boldsymbol{\tau}$—viscous stress tensor,
$\boldsymbol{g}$—gravity acceleration (m/s^2),
$\boldsymbol{F_s}$—surface tension source term, which adopts CSF model (Continuum Surface Force):

$$\boldsymbol{F_s} = \sigma\kappa(\phi)\nabla H(\phi), \tag{8}$$

σ—surface tension coefficient (N/m),
$H(\phi)$—Heaviside function, which is introduced to smooth the density and viscosity at the interface [18]:

$$H(\phi) = \begin{cases} 1, & \phi \geq +h \\ 0, & \phi \leq -h \\ 0.5 + \phi/3h & \\ \quad + \sin[2\pi\phi/3h]/2\pi, & |\phi| \leq h \end{cases}, \tag{9}$$

h—the mesh size (mm),
$\boldsymbol{S}$—the strain rate tensor:

$$\boldsymbol{S} = \frac{1}{2}\left[\nabla \boldsymbol{u} + (\nabla \boldsymbol{u})^T\right], \tag{10}$$

Then the different regions density ρ and viscosity μ can be calculated by Heaviside function:

$$\rho(\phi) = \rho_l[1 - H(\phi)] + \rho_g H(\phi), \tag{11}$$

$$\mu(\phi) = \mu_l[1 - H(\phi)] + \mu_g H(\phi), \tag{12}$$

ρ_l—liquid phase density (kg/m^3),
ρ_g—gas phase density (kg/m^3),
μ_l—liquid phase viscosity (Pa·s),
μ_g—gas phase viscosity (Pa·s).

The energy equation is as follows:

$$\partial \rho c_p T/\partial t + \nabla(\rho c_p T \boldsymbol{u}) = \nabla \bullet \lambda \nabla T, \tag{13}$$

T—the temperature (K),
λ—the thermal conductivity (W/(K·m)),
c_p—the heat capacity (J/(kg·K)).

2.2.2. Evaporation Model

The boiling point of liquid nitrogen is relatively low. When the liquid nitrogen drops impact the wall at room temperature, violent phase transition is inevitable, and the evaporation process should be considered by Lee's [20] model:

$$\dot{m}_g = A\alpha_l\rho_l\frac{T - T_{sat}}{T_{sat}}, T > T_{sat}, \tag{14}$$

$\dot{m}_g$—the phase change rate of the gas phase (kg·m^{-3}·s^{-1}),
α_l—the volume fraction of the liquid phase,
T_{sat}—the saturation temperature (K),
A—the factor controlling the phase change, A is set to 0.1 s^{-1} in this paper.

2.3. Model Setup and Mesh Independence Verification

A two-dimensional physical model of single liquid nitrogen droplet impacting the wall surface is shown in Figure 1. The boundary conditions are listed below: the initial diameter is D_0, the initial velocity is U_0, the velocity direction is vertically downward, the ambient pressure is 0.1 MPa, wall temperature T_w = 300 K, the static contact angle θ = 90°. The ambient gas is nitrogen, the top and sides are the pressure outlet boundaries, and the bottom is a non-slip wall surface. In order to facilitate the analysis of the transient process after the liquid nitrogen droplet hits the wall, it is assumed that the initial droplet is

spherical, and the bottom of the droplet is tangent to the wall at the initial time. The thermal radiation effect is ignored in this model and both gas and liquid phases are incompressible fluids. The software Fluent 17.0 is used to solve the numerical model. The governing equation is discretized using the finite volume method. The coupling of pressure and velocity is based on the Coupled method. The pressure is solved using the PRESTO method. The QUICK algorithm is used to solve the Level Set equation. The momentum and energy equations adapt a second-order upwind, with a time step $\Delta t = 10^{-6}$ s, and the number of iterations in Δt is 20.

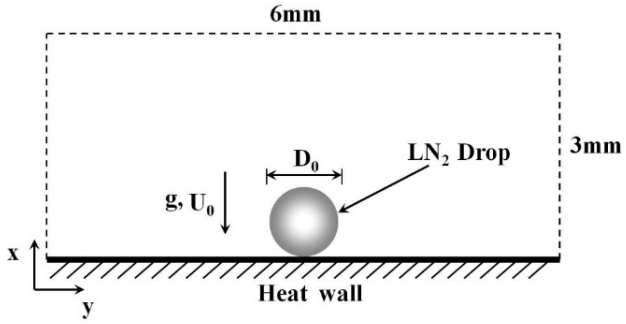


Figure 1. Model of droplet impact on wall at initial time.

The quadrangular structured grids of 200 × 400, 250 × 500, 300 × 600, and 350 × 700 are used for grid independence verification, respectively (impact parameters: U_0 = 0.1 m/s, D_0 = 0.5 mm, T_w = 300 K, θ = 90°); the droplet spreading factor β is defined as the ratio of the droplet spreading diameter D_t to the initial droplet diameter D_0. The relationship between the spreading factor β of the four grids over time is shown in Figure 2. It can be seen that as the number of grids increases, the spreading factor β gradually increases. When the number of grids reaches 300 × 600, the number of grids has little effect on the spreading diameter. Considering the calculation accuracy and calculation efficiency comprehensively, grids with mesh size of 300 × 600 are applied in the simulations below.

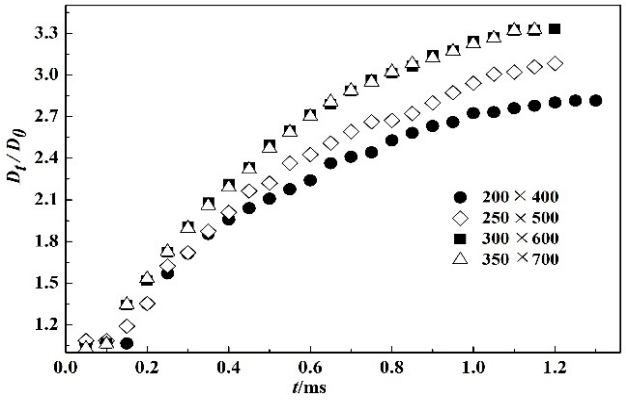


Figure 2. Verification of grid independence.

2.4. Model Validation

In the practical liquid nitrogen spray cooling process, the distance between the nozzle and the wall surface is relatively short, and the initial velocity of liquid nitrogen drops is relatively large; hence, the liquid nitrogen droplets will not completely evaporate before droplets hit the wall surface. Chandra and Aziz [16] verified this hypothesis through experiments at normal temperature and pressure: they dropped the liquid nitrogen with D_0 = 1.9 mm freely from the copper surface by 27 mm, and found that the life of the liquid nitrogen droplet on the copper surface was about 8.2 s, while the maximum impact time scale $t^* = D_0/U_0$ = 7 ms. The results showed that the time scale of droplet evaporation is much larger than the time scale of droplet impact.

For quantitative validation of numerical models, a group of experimental data are selected from Hatta et al. [21] (T_w = 773 K, D_0 = 2 mm, initial water drop temperature 293 K, U_0 = 2.05 m/s, static contact angle θ = 57°), and the relevant parameters used in the simulation process are shown in Table 1. The calculated results and the experimental results are shown in Figure 3. It can be seen that as the impact process continues, the spreading factor increases first and then tends to be gentle, and the simulation results are basically consistent with the experimental results. Therefore, the results in Figure 3 quantitatively verify the validity of the numerical model.

Table 1. Related parameters.

Parameters	Value
Liquid nitrogen density (kg/m^3)	806.88
Liquid nitrogen surface tension coefficient (N/m)	8.22×10^{-3}
Liquid nitrogen viscosity (Pa·s)	160.08×10^{-6}
Initial velocity of liquid nitrogen drop (m/s)	0.1~5
Initial diameter of liquid nitrogen drop (mm)	0.2~0.7
Initial temperature of liquid nitrogen drop (K)	78
Wall surface temperature (K)	100~400
We	0.20~1716

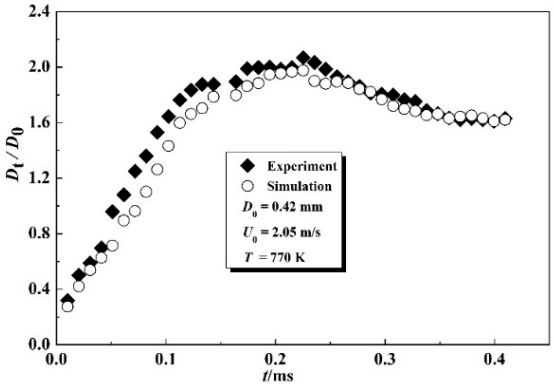


Figure 3. Comparison of experimental and simulated results.

To qualitatively verify the numerical model, the experimental data (T_w = 657 K, D_0 = 2 mm, initial droplet temperature 293 K, *We* = 2) from Liang et al. [22] are selected. The morphological evolution of numerical results (up) and experimental results (down) are shown in Figure 4. It can be seen that the liquid droplet has experienced spreading, retraction, and rebound after impinging the wall surface. The simulation results are in good agreement with the experimental results. It shows that it is feasible to establish a physical model of liquid nitrogen droplet impacting on the wall surface with a certain initial velocity and diameter.

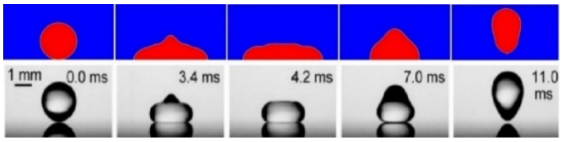


Figure 4. Droplet morphology evolution comparison between experimental and simulated results.

3. Results and Discussions

3.1. The Effect of Initial Velocity and Diameter of Droplets

Droplet diameter and velocity are important atomization parameters of spray cooling. As shown in Figure 5, when the liquid nitrogen droplets impact the wall surface with different diameters and velocities, there appear three spreading behaviors: rebound, retraction,

and splashing, which are very similar to the spreading behaviors of diesel droplet [23] and water droplet [24] impacting the high-temperature wall surface ($T_w > T_{DL}$).

When D_0 = 0.2 mm, U_0 = 0.1 m/s, at the initial stage (t = 0.1 ms) the bottom of the droplet has a short contact with the wall surface, the large temperature difference causes violent phase change at the bottom of the droplet, and then the small cavity is formed at the bottom of the droplet. Wu et al. [25] also observed the cavity at the bottom of the droplet. When t = 0.3 ms, the droplet spread reaches its maximum diameter and suspends above the wall surface, the droplet begins to retract to form an arc-shaped liquid film at 0.5 ms, and rebounds away from the wall surface at 0.8 ms. This process can be called rebound.

When D_0 = 0.5 mm, U_0 = 0.1 m/s, the cavity also appeared at the bottom of the droplet at 0.01 ms. With the continuous impact process, the cavity gradually became larger. The droplet expands into a disk-shaped liquid film with bulge in the middle, the wall and the liquid film are separated by a vapor film (1 ms), the liquid film begins to retract and a very thin liquid film area appears in the neck, the two edge thin liquid films break in the neck, then forming two secondary small droplets (1.2 ms), but the middle part of the liquid film continues to retract until 2.5 ms. The process can be regarded as retraction.

When D_0 = 0.5 mm and U_0 = 5 m/s, comparing with the above two spreading behaviors, the droplet spreading shape changes greatly, no cavity is observed at the bottom of the droplet at the beginning of the impact, many secondary small droplets appear on the edge, and splash outward at 0.08 ms. As the impact process continues, part of the liquid in the center is still in continuous contact with the wall surface (0.4 ms), and the droplet breaks completely within 0.8 ms, finally forming a chain-like droplet group. This spreading process is recorded as splashing. However, the occurrence of splashing means the loss of cooling medium, which is unfavorable for improving the refrigerant utilization.

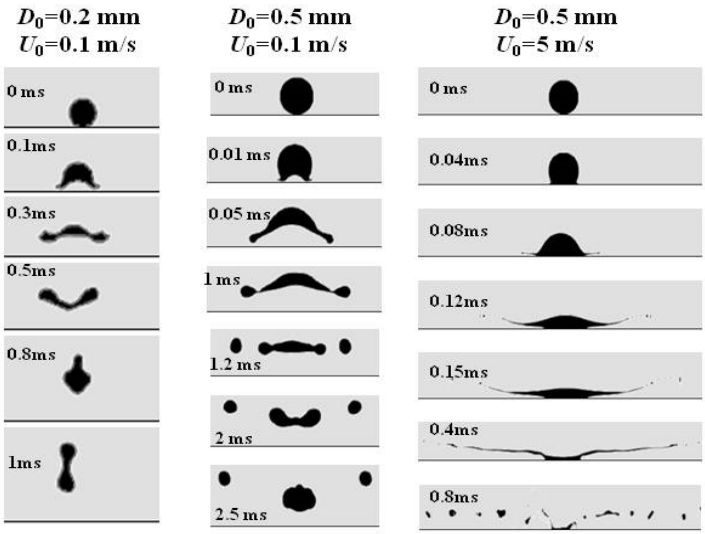


Figure 5. Droplet spreading patterns under different initial impacting conditions.

Park et al. [26] found that increasing the D_0 (2 to 2.3 mm) and U_0 (0.08 to 2.36 m/s) of the droplets had a positive effect on the spreading factor. The increase of the spreading factor means that the thinner the thickness of the liquid droplet deposited as a disc on the wall surface, the more the corresponding heat transfer resistance decreases, and heat transfer area increases, which is beneficial to improving the cooling efficiency. Thus, the impact velocity and diameter of liquid nitrogen droplets are the key parameters that affect the utilization of working fluid and heat transfer efficiency. It can be seen from Figure 6 that the spreading factors of the three spreading behaviors (rebound, retraction, splashing) vary greatly with time. For the droplet with small particle size and low velocity (D_0 = 0.2 mm, U_0 = 0.1 m/s), the inertial force is small and the surface tension plays a primary role, the kinetic energy of the droplet during retraction is greater than the sum of the viscosity loss and the surface energy of the droplet. The reverse pressure of the vapor drives the liquid droplet to

bounce off the wall surface, thus the spreading factor β shows a tendency of increasing first and then decreasing. As the diameter of the droplet increases (D_0 = 0.5 mm, U_0 = 0.1 m/s), the β increased to the maximum at 1.2 ms, and then the increasing trend weakens, which corresponds the droplet begins to retract after spreading to the maximum and then breaks at the neck. When the droplet velocity is large enough (D_0 = 0.5 mm, U_0 = 5 m/s), the spreading factor of splashing is much higher than the rebound and retraction. Due to the rapid increase of the kinetic energy of the droplet, the edge liquid detaches fast from the mother droplet and forms secondary sporadic droplets. The small secondary droplets on the edges will move upward due to the surrounding gas blocking, which leads to a decrease in the spreading factor at 0.8 ms. The analysis suggests that both increasing D_0 and U_0 results in an increase in the kinetic energy of the droplet, which means that the droplet has sufficient energy to overcome the adverse effects of flow resistance, thereby significantly increasing the spreading factor. Apparently, increasing the impact velocity of the droplet has a greater influence on the spreading behaviors than droplet diameter.

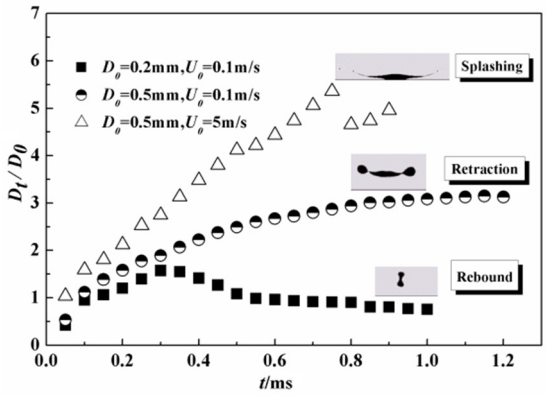


Figure 6. Curves of droplet spreading patterns under different initial impacting conditions.

3.2. The Effect of Wall Temperature

Figure 7 shows the spreading process of 0.5 mm liquid nitrogen droplet hitting different temperature walls (100, 200, and 400 K) with the velocity 0.1 m/s. As can be seen from Figures 5 and 7, the wall temperature has a significant influence on the spreading behavior of the liquid nitrogen droplets. The spreading process of liquid nitrogen droplets on the wall at temperatures of 200, 300, and 400 K is relatively similar, the small cavity is formed at the bottom of the droplet at the beginning, and both of them break into multiple small droplets during the process of retraction.

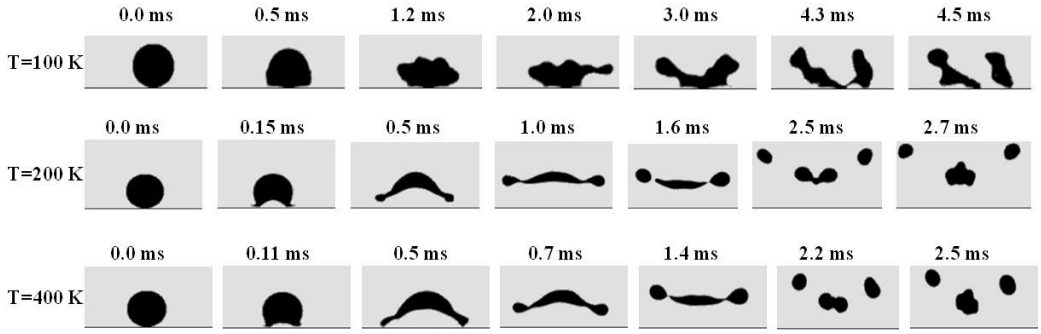


Figure 7. The spreading process of droplets impinging on different temperature walls.

However, on the 100 K wall, the spreading behaviors changes significantly. No cavities are observed at the bottom of the droplet at the beginning of impact (0.5 ms), and the Leidenfrost phenomenon did not occur. The bottom of the droplet continues to contact the wall surface during the subsequent spreading process (2.0 ms). This is because the wall temperature is close to the T_{DL} of liquid nitrogen, and the vapor reverse pressure is

not enough to support the droplets to suspend on the wall. In the following spreading process, the droplets spread irregularly along the radial direction on the wall. Almost all the kinetic energy is converted into surface energy at 3.0 ms, and the droplet begins to retract. Finally, at 4.5 ms, the bottom of the droplet is completely evaporated. Tran T et al. [24] experimentally found that when the wall temperature is close to T_{DL}, the stable gas film cannot be formed between the droplet and the wall; thereby, the contact boiling occurs. As the temperature rises, the Leidenfrost effect begins to appear. The experimental results of Tran T et al. [24] well verify the accuracy of the numerical simulation results in this paper.

To further investigate the influence of wall temperature on the spreading factor, Figure 8 shows the curves of spreading factor with time when the 0.5 mm liquid nitrogen droplet hits the wall at different temperatures (100, 200, 300, 400 K) with the initial velocity 0.1 m/s and 0.5 m/s. It can be seen from Figure 8 that the spreading factors at the two impact velocities both increase with the increase of the wall temperature. Further analysis of Figure 8a,b shows that when the impact velocity increases from 0.1 m/s to 0.5 m/s, the spreading behavior of the droplets on the different temperature walls change from retraction to splashing. It means that the dominant parameter for the spreading state of the droplet is still the droplet impact velocity. The increase of wall temperature ($T_W > T_{DL}$) directly affects whether the gas film between the wall and the droplet can be formed [24,25]. The existence of the gas film reduces the energy dissipation during the spreading process, thereby accelerating the spreading of the droplets on the wall [27]. In addition, the viscosity of the liquid on the high temperature wall is reduced, which is also conducive to the spreading of droplets. Therefore, increasing the wall temperature can not only accelerate the droplets spreading and reduce the thermal resistance, it can also increase the temperature difference between the wall and the fluid [17], thereby increasing the heat flux.

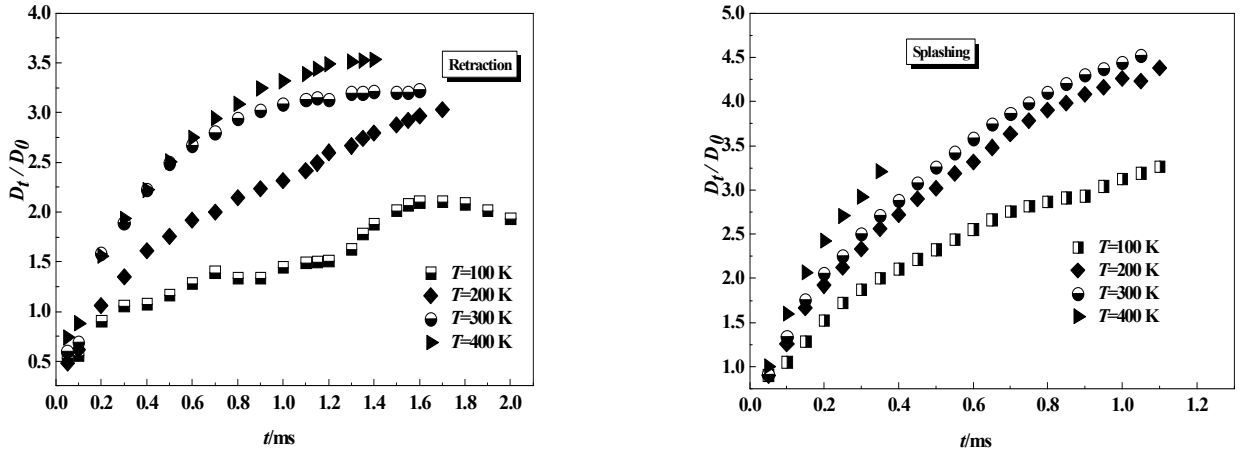


Figure 8. Curves of spreading factor with time at different wall temperatures, (**a**) 0.1 m/s; (**b**) 0.5 m/s.

3.3. The Effect of We

The impact process is essentially the conversion of kinetic energy and surface energy; *We* represents the relative size of the kinetic energy and surface energy of the droplet, and the expression is as follows:

$$We = \rho U_0^2 D_0 / \sigma, \quad (15)$$

Figure 9 shows the curves of the spreading factor over time (T_w = 300 K) under different *We*. It can be seen that as *We* gradually increases, in the initial stage of impact, the inertial force gradually plays a leading role, and the droplet has enough energy to overcome the obstacle of surface tension, so that droplet spreads rapidly along the radial direction on the wall, the spreading factor is increased accordingly. With the increase of *We*, within a certain range, the rebound (*We* < 0.2), retraction (0.2 < *We* < 4.9), and splashing

(*We* > 4.9) occur in order. Zhang et al. [23] found that when tiny diesel droplets hit high temperature wall surface, three states of rebound (*We* < 20), retraction (20 < *We* < 80), and splashing (*We* > 80) also occurred in the different range of *We*. Obviously, the critical transition conditions for judging the evolution of liquid nitrogen droplet morphology is quite different from that of diesel droplet. This may be because liquid nitrogen is a highly wetting fluid. It means that with the same *We* number, liquid nitrogen consumes more energy during the process of radial expansion and retraction, and thus the critical conditions of liquid nitrogen droplet rebound, retraction, and splashing are smaller. Liang et al. [27] found that the critical conditions of butanol are also significantly lower than those working fluids such as water and diesel, and even the heptane droplets did not observe the phenomenon of rebound under all experimental conditions. It proves that the critical transition conditions are closely related to the physical properties of the droplets, especially the viscosity of liquid.

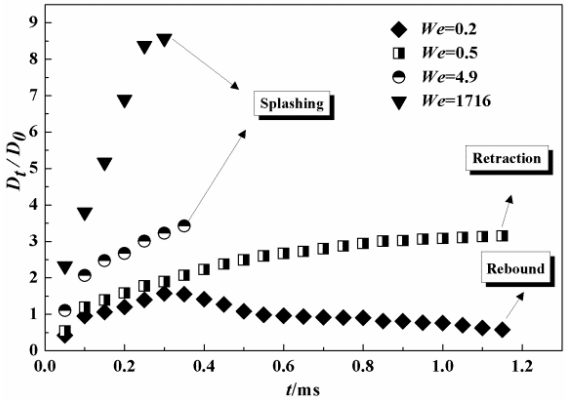


Figure 9. Curves of spreading factor with time under different *We* conditions.

The maximum spreading factor γ is defined as the ratio of the maximum spreading diameter D_{max} to the initial diameter D_0 of the droplet. Many studies have shown that there is a power correlation between the maximum droplet spreading factor and *We*, and the model $D_{max}/D_0 \sim We^{1/4}$ has a wide adaptability [3,4,28]. The liquid nitrogen droplets impacting the wall surfaces (300 K) with a large range of *We* (0.20~1717) are fitted and the fitting result is shown in Figure 10, and it can be seen that D_{max}/D_0 has a power relationship with *We*:

$$D_{max}/D_0 = 0.789We^{0.306} + 2.64, \quad (16)$$

In relation to the power exponent of the fitting results in this paper $\varepsilon = 0.306 > 0.25$, Tran [10] also found a similar phenomenon ($\varepsilon = 0.39 > 0.25$). He even found that when using various droplets such as FC-72, water, and ethanol to hit hydrophilic, hydrophobic, and superhydrophobic walls, the power indexes are always between 1/4 and 1/2, which is consistent with the simulation results in this paper. The possible reasons for the increase of power index are (1) the large temperature difference between the liquid nitrogen and the wall surface causes the vapor generated rapidly, and accompanied by the violent ejection of the liquid radically outward; (2) liquid nitrogen is a highly wetting fluid, a smaller *We* can obtain a larger spreading diameter.

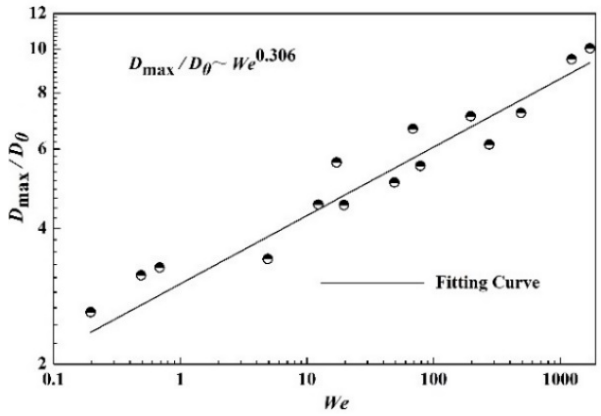


Figure 10. The relationship between the maximum spreading factor D_{max}/D_0 and *We*.

4. Conclusions

The mature application of liquid nitrogen spray cooling technology is of positive significance to promoting the sustainable development of the refrigeration industry. In this paper, the detailed process of liquid nitrogen droplet impacting the wall is studied by numerical method. The main conclusions are as follows:

(1) When liquid nitrogen droplets hit the wall surface ($T_w > T_{DL}$), there are three movement states: rebound, retraction, and splashing, which are very similar to the general spreading behavior of ordinary working fluids.

(2) Increasing the diameter and velocity of droplet is beneficial to increase the droplet spreading factor, and the impact velocity has more significant effect on spreading behaviors.

(3) When the wall temperature approaching the Leidenfrost temperature ($T_w \approx T_{DL}$), the bottom of the liquid nitrogen droplet is in constant contact with the wall and spreads irregularly. The viscosity of the droplet decreases with the increase of the wall temperature, and a vapor film between the droplet and the wall is formed, which promotes the spreading of the droplet.

(4) Due to the large difference between the physical properties of liquid nitrogen and normal working fluids, the critical conditions for droplet breakup and rebound have changed; the maximum spreading factor has a power correlation with *We*.

For liquid nitrogen spray cooling, attention should be paid to controlling the impact parameters of the droplets. Although increasing the impact velocity can inhibit the formation of the vapor film, thereby enhancing the heat transfer performance, the violent splash phenomenon will also result in the loss of the refrigerant, which in turn will cause a decrease in the refrigerant utilization rate. Therefore, the performed simulations suggest that providing sufficient fresh droplets and continuously impacting the wall surface at a certain velocity are effective means to improve the cooling efficiency of liquid nitrogen spray.

Author Contributions: Conceptualization, K.Z.; methodology, Y.D.; software, K.Z.; validation, K.Z. and Y.D.; formal analysis, K.Z. and Y.D.; investigation, Y.D.; resources, K.Z. and Y.D.; data curation, K.Z. and Y.D.; writing—original draft preparation, K.Z.; writing—review and editing, Y.D.; visualization, K.Z. and Y.D.; supervision, Y.D.; project administration, K.Z. and Y.D.; funding acquisition, K.Z. and Y.D. All authors have read and agreed to the published version of the manuscript.

Funding: This research was funded by the Natural Science Foundation of the Jiangsu Higher Education institutions of China, grant number 18KJB560007 and the Research Fund of Key Laboratory of Aircraft Environment Control and Life Support, MIIT, Nanjing University of Aeronautics and Astronautics, grant number KLAECLS-E-201902, Natural Science Research Project of Anhui Provincial Department of Education, grant number KJ2018B16.

Institutional Review Board Statement: Not applicable.

Informed Consent Statement: Not applicable.

Data Availability Statement: Not applicable.

Acknowledgments: The authors acknowledge the Natural Science Foundation of the Jiangsu Higher Education institutions of China and the Research Fund of Key Laboratory of Aircraft Environment Control and Life Support, MIIT, Nanjing University of Aeronautics and Astronautics, Natural Science Research Project of Anhui Provincial Department of Education.

Conflicts of Interest: The authors declare no conflict of interest.

References

1. Chai, Y.; Lin, X.; Wang, D. Industrial Structure Transformation and Layout Optimization of Beijing-Tianjin-Hebei Region under Carbon Emission Constraints. *Sustainability* **2021**, *13*, 643. [CrossRef]
2. Bayar, Y.; Gavriletea, M.; Sauer, S.; Paun, D. Impact of Municipal Waste Recycling and Renewable Energy Consumption on CO_2 Emissions across the European Union (EU) Member Countries. *Sustainability* **2021**, *13*, 656. [CrossRef]
3. Liang, G.; Mudawar, I. Review of spray cooling—Part 1: Single-phase and nucleate boiling regimes, and critical heat flux. *Int. J. Heat Mass Transf.* **2017**, *115*, 1174–1205. [CrossRef]
4. Biance, A.-L.; Pirat, C.; Ybert, C. Drop fragmentation due to hole formation during Leidenfrost impact. *Phys. Fluids* **2011**, *23*, 22104. [CrossRef]
5. Gao, X.; Li, R. Impact of a single drop on a flowing liquid film. *Phys. Rev. E* **2015**, *92*, 053005. [CrossRef]
6. Wachters, L.; Smulders, L.; Vermeulen, J.; Kleiweg, H. The heat transfer from a hot wall to impinging mist droplets in the spheroidal state. *Chem. Eng. Sci.* **1966**, *21*, 1231–1238. [CrossRef]
7. Baumeister, K.J.; Simon, F.F. Leidenfrost Temperature—Its Correlation for Liquid Metals, Cryogens, Hydrocarbons, and Water. *J. Heat Transf.* **1973**, *95*, 166–173. [CrossRef]
8. Scheller, B.L.; Bousfield, D.W. Newtonian drop impact with a solid surface. *AIChE J.* **1995**, *41*, 1357–1367. [CrossRef]
9. Liu, H.; Shen, X.; Wang, R.; Cao, Y.; Wang, J. Study on spreading characteristics of nanofluids droplet impinging on solid surface. *Acta Mech. Sin.* **2018**, *50*, 1024–1031.
10. Tran, T.; Staat, H.J.J.; Prosperetti, A.; Sun, C.; Lohse, D. Drop Impact on Superheated Surfaces. *Phys. Rev. Lett.* **2012**, *108*, 036101. [CrossRef] [PubMed]
11. Ming, C.; Jing, L. Lattice Boltzmann simulation of a drop impact on a moving wall with a liquid film. *Comput. Math. Appl.* **2014**, *67*, 307–317. [CrossRef]
12. Breitenbach, J.; Roisman, I.; Tropea, C. From drop impact physics to spray cooling models: A critical review. *Exp. Fluids* **2018**, *59*, 55. [CrossRef]
13. Celestini, F.; Kirstetter, G. Effect of an electric field on a Leidenfrost droplet. *Soft Matter* **2012**, *8*, 5992–5995. [CrossRef]
14. Liang, G.; Mudawar, I. Review of spray cooling—Part 2: High temperature boiling regimes and quenching applications. *Int. J. Heat Mass Transf.* **2017**, *115*, 1206–1222. [CrossRef]
15. Liang, G.; Mudawar, I. Review of drop impact on heated walls. *Int. J. Heat Mass Transf.* **2017**, *106*, 103–126. [CrossRef]
16. Zhao, K.; Wang, Y.; Ding, Y.; Jiang, Y. Numerical and theoretical study on the spreading characteristics of droplet impact on a horizontal flowing liquid film. *Colloids Surfaces A Physicochem. Eng. Asp.* **2021**, *616*, 126338. [CrossRef]
17. Zhao, K.; She, Y.-Z.; Jiang, Y.-L.; Qin, J.; Zhang, Z.-H. Numerical study on phase change behavior of liquid nitrogen droplets impinging on solid surface. *Acta Phys. Sin.* **2019**, *68*, 244401. [CrossRef]
18. Wang, Y.-B.; Wang, X.-D.; Wang, T.-H.; Yan, W.-M. Asymmetric heat transfer characteristics of a double droplet impact on a moving liquid film. *Int. J. Heat Mass Transf.* **2018**, *126*, 649–659. [CrossRef]
19. Lee, W. *Pressure Iteration Scheme for Two-Phase Flow Modeling*; Hemisphere Publishing: Washington, DC, USA, 1980.
20. Chandra, S.; Aziz, S.D. Leidenfrost Evaporation of Liquid Nitrogen Droplets. *J. Heat Transf.* **1994**, *116*, 999–1006. [CrossRef]
21. Hatta, N.; Fujimoto, H.; Kinoshita, K.; Takuda, H. Experimental Study of Deformation Mechanism of a Water Droplet Impinging on Hot Metallic Surfaces Above the Leidenfrost Temperature. *J. Fluids Eng.* **1997**, *119*, 692–699. [CrossRef]
22. Liang, G.; Shen, S.; Guo, Y.; Zhang, J. Boiling from liquid drops impact on a heated wall. *Int. J. Heat Mass Transf.* **2016**, *100*, 48–57. [CrossRef]
23. Zhang, Y.; Ning, Z.; Lv, M.; Sun, C. Dynamics of droplet impacting onto heated surface. *J. Combust. Sci. Technol.* **2017**, *5*, 451–457.
24. Tran, T.; Staat, H.J.J.; Susarrey-Arce, A.; Foertsch, T.C.; van Houselt, A.; Gardeniers, H.J.G.E.; Prosperetti, A.; Lohse, D.; Sun, C. Droplet impact on superheated micro-structured surfaces. *Soft Matter* **2013**, *9*, 3272–3282. [CrossRef]
25. Wu, S.; Zhang, C.; Chen, Y.; Shi, M. Phase change behavior of the droplet impingement on a hot surface. *J. Eng. Thermophys.* **2018**, *39*, 174–177.
26. Park, H.; Carr, W.W.; Zhu, J.; Morris, J.F. Single drop impaction on a solid surface. *AIChE J.* **2003**, *49*, 2461–2471. [CrossRef]
27. Liang, G.; Yang, Y.; Guo, Y.; Zhen, N.; Shen, S. Rebound and spreading during a drop impact on wetted cylinders. *Exp. Therm. Fluid Sci.* **2014**, *52*, 97–103. [CrossRef]
28. Antonini, C.; Amirfazli, A.; Marengo, M. Drop impact and wettability: From hydrophilic to superhydrophobic surfaces. *Phys. Fluids* **2012**, *24*, 102104. [CrossRef]